

One-way Ranging for Mobile Underwater Acoustic Networks with Long Interaction Periods

Jianyu Zhang, Filippo Campagnaro, Antonio Montanari, Michele Zorzi

Department of Information Engineering, University of Padova, Italy
{campagn1,montanar,zorzi}@dei.unipd.it, jianyu.zhang@studenti.unipd.it

Abstract—One of the main challenges in underwater positioning is a correct estimate of the sound speed in the deployment area. In fact sound speed can be either directly measured with a velocity meter, or indirectly computed from Conductivity Temperature and Depth (CTD) measurements. While the former approach requires the use of very precise devices that need to be often calibrated, the latter requires the use of extremely precise CTDs that are usually very expensive. The availability of low-cost unmanned underwater vehicles and low-cost acoustic modems makes the integration of both velocity meters and CTDs impractical, as the cost of these devices will be in the same order of magnitude of the unmanned vehicle itself. On the other hand, the recent availability of large data-sets of sound speed measurements in various parts of the world, and the efficient implementation of Machine Learning algorithms that can nowadays run also in embedded devices, suggest a new approach based on sound speed prediction through Machine Learning algorithms trained on historical data of sound speed and environmental measurements in the area close to the deployment.

In this paper we analyze a different approach for this prediction, and assess the effect of a wrong sound speed estimate in our newly proposed ranging protocol developed in the DESERT Underwater Framework.

Index Terms—Ranging, underwater acoustic networks, sound speed profile prediction, DESERT Underwater.

I. INTRODUCTION

The ocean contains a vast amount of resources: mineral, biological, ecological, defense, and is a unique physical environment for researchers to test various ideas. To gradually obtain resources and utilize the physical environment of the ocean, people are gathering all their strength to go deep into it. Unmanned underwater swarms are currently a popular means of safely exploring the ocean on a large scale [1]. In underwater unmanned swarms, applications such as mobile formation maintenance, joint detection and sensing, joint mobile positioning and path planning, acoustic-optic image data splicing and data fusion require more flexible, convenient and accurate ranging between mobile sensing units [2], [3]. Since optical signals and electromagnetic signals are severely attenuated underwater, and the cost of additional ranging sensors is too high, in underwater unmanned swarms equipped with underwater acoustic communication devices we prefer to integrate the ranging function into communication networks.

The basic principles of underwater ranging are the same as in terrestrial ranging [4], while the following differences need

to be considered in the design. The speed of sound is five orders of magnitude lower than the speed of electromagnetic signals, so the impact of node mobility is more pronounced than on land. In fact, we must consider the movement of nodes during the propagation delay, and underwater Doppler shift increases significantly due to the low propagation speed of acoustic signals. The speed of sound under water is also affected by temperature, salinity and pressure, which vary with depth, location, environmental conditions, time of the year and hour of the day [5]. Underwater acoustic spectrum resources are limited, and the occupation of channel resources by ranging applications must be coordinated through the underwater Medium Access Control (MAC) protocol, making it difficult to ensure that ranging services are available in real time.

Based on the above considerations, we have added improvements suitable for modern underwater acoustic networks to the existing ranging algorithm to achieve the goals of being low-cost, accurate and suitable for applications.

The first contribution of this paper is to propose a real-time sound velocity estimation method that does not rely on Conductivity Temperature and Depth (CTD) sensors [6] and sound velocity meters [7] to improve the accuracy of ranging without increasing costs. In fact, both devices have a price in the same order of magnitude of low-cost Autonomous Underwater Vehicles (AUVs) and Remotely Operated Vehicles (ROVs), making them unusable in low-cost swarm deployments. Our approach, instead, relies on applying Machine Learning algorithms to predict the sound speed profile in a certain location and in a certain time of the year. The algorithm will be trained with historical CTD and environmental data publicly available online. Different prediction approaches are compared and the impact of a good and bad prediction analyzed in a newly developed ranging algorithm.

The second contribution of this paper is the design of a novel ranging protocol for underwater networks. We adopt a one-way ranging method to adapt to the underwater MAC protocol. Single packet ranging can be better integrated into various network topologies and application scenarios, providing more flexible services. At the same time, it reduces signaling overhead and channel occupancy, and also reduces interference to surrounding acoustic systems. Moreover, the existence of low-cost Oven-Controlled Crystal Oscillators (OCXO) [8] enables precise clock synchronization without the need for expensive atomic clocks. Different from traditional one-way ranging methods, we exploit the node movement information hidden

F. Campagnaro, corresponding author (email: campagn1@dei.unipd.it), is with the Department of Information Engineering, University of Padova, Italy. This work was supported in part by the FSE REACT EU, PON Research and Innovation 2014-2020 (DM 1062/2021), PNRR DM 352 scholarship and by China Scholarship Council (CSC) under the Grant CSC N°202008220156.

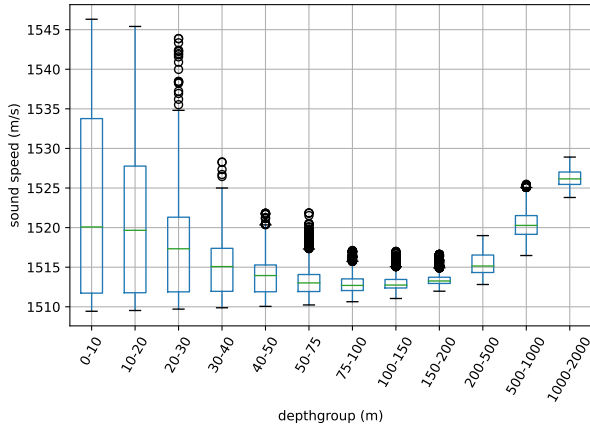


Fig. 1: Sound speed variability observed for almost 4 years at different water depth.

in communication packets. Based on the sending timestamp, arrival time and stop receiving time of two consecutive packets of the same duration in one transmission, we can infer the speed and movement trajectory of the mobile node. We divide one-way ranging into active and passive, uplink and downlink situations, and propose corresponding calculation methods respectively, to adapt to different network topologies and network applications. This protocol is implemented and evaluated in a realistic scenario by means of the DESERT Underwater network simulator [9].

This paper is structured as follows. Section II presents the sound speed prediction algorithms and discusses its precision. Section III details a novel one-way ranging protocol for underwater networks. The protocol is then evaluated in Section IV. Section V finally concludes the paper.

II. SOUND SPEED PREDICTION

The underwater acoustic channel is affected by seawater pressure, temperature and salinity, and the propagation path is curved and complicated. Moreover, underwater acoustic channels present a complex distribution of sea areas, latitudes, seasons and depths. The underwater acoustic channel has a high degree of space-time variation. Without these hydrometeorological parameters, the establishment of the underwater acoustic channel is extremely unreliable. Considering the high cost of deploying sensor nodes and conducting ocean exploration, it is necessary to predict the sound velocity profile of the target sea area in the target time window in advance to estimate the state of the underwater acoustic channel. The boxplots in Figure 1 highlights how the sound speed changes during 4 years at different water depth. While in deep water the maximum variability is between 5 and 10 m/s, in shallow water the sound speed can change quite significantly, with a maximum variability that can even exceed 30 m/s during the year.

In Section II-A we present the data-set used for training our prediction algorithms, which is explained in Section II-B and evaluated in Section II-C.

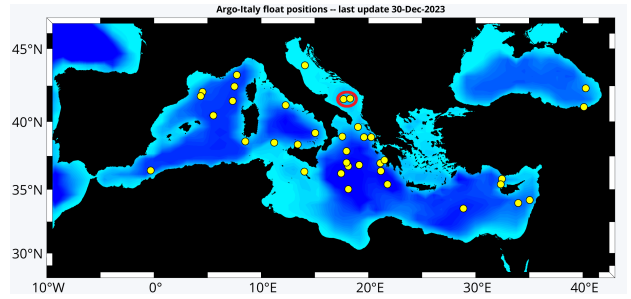


Fig. 2: Last positions of active Argo-Italy floats, image from [12].

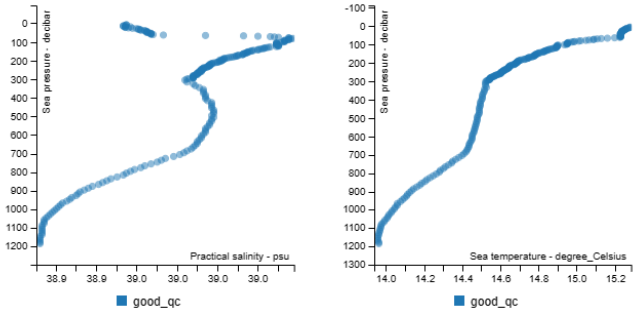


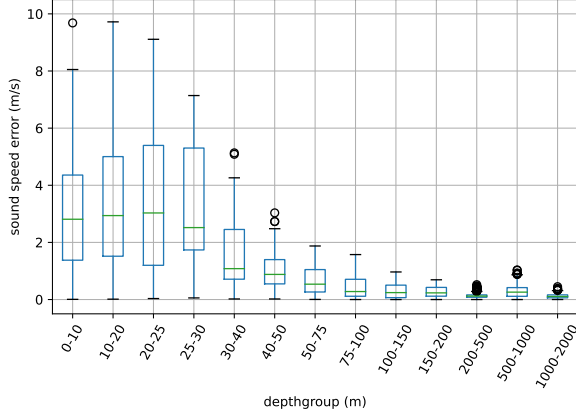
Fig. 3: Argo data (salinity and temperature) for floater 6903799 acquired on the 22nd of December 2023.

A. Argo Data-Set

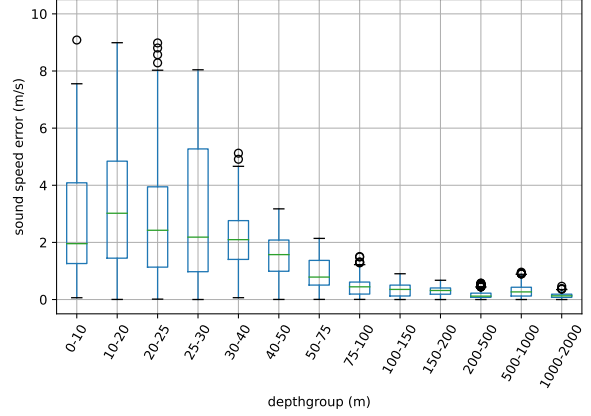
The Argo program [10] collects various data with more than 3'500 floats deployed across the world's oceans, describing the temperature and salinity of the water, and some of them also measure other properties that describe the biology/chemistry of the ocean. These data were collected and made freely available by the International Argo Program and the national programs that contribute to it. The Argo Program is part of the Global Ocean Observing System [11], and more than 100'000 temperature and salinity profiles are collected each year.

In this paper we focus on the data acquired by Argo-Italy [12], which focuses mainly on the Mediterranean sea: the position of the floaters can be observed in Figure 2: for our prediction model we focus on the data retrieved by the two floaters highlighted in red at the center of the map and located between Italy and Albania. The floaters unique identifiers are 6903799 and 6903825, respectively. From these two floaters, a data measurement cycle is performed every 5 days. To date, 215 measurement cycles are available for floater 6903799, while 80 cycles are available for floater 6903825. An example of temperature and salinity profile downloaded from the Argo website is depicted in Figure 3.

In this paper, we try to predict the spatial-temporal variation of the target sea area with the Argo data-set. In the Argo data frame, we can obtain various hydrometeorological parameters of different water depths sampled by the buoy in each previous round of missions, as well as the timestamp and precise coordinates of each data upload.



(a) Error of a single RF trained with all data.



(b) Error when two RF are used to predict deep and shallow water.

Fig. 4: Boxplots grouped by depth showing the error of the prediction models.

B. Sound Speed Prediction Algorithm

Water temperature changes are mainly determined by location, depth and salinity, hence these three parameters are used for training our prediction model. We chose to use the random forest algorithm, that in [13] was proven to be a valuable choice to predict sound speed in the Pacific Ocean. A random forest regression, in fact, is a supervised learning algorithm that uses an ensemble learning method. Specifically, it creates a group of decision trees from different samples of input data. For regression tasks, it returns the mean or average prediction of the individual trees. It is a bagging technique that reduces the variance and works well for most kinds of data. In contrast to neural networks, random forests are less accurate, but require less data for training and are less computationally expensive, making them a good fit for battery-supplied low-cost vehicles deployment. In this paper, we trained the random forest with time, depth and salinity measured in the last 42 months.

We highlight that the Argo measurements are provided with a quality metrics. Low quality measurements refer to samples taken in unstable conditions or temporary malfunctioning of the sensory system, and are not used in the training process.

Given the depth d and from the prediction of salinity s and temperature t we can compute the sound speed c with the Wilson equation [14]:

$$c(t, s, d) = 1449.2 + 4.6t - 0.055t^2 + 0.017d + (1.34 - 0.01t)(s - 35). \quad (1)$$

C. Sound Speed Prediction Accuracy

In this section, we discuss the accuracy of the random forest (RF) model described in Section II-B. Specifically, we trained the random forest with 42 months of data, and then predict the next 4 months (from July to October 2023).

Table I shows the Mean Absolute Error and prediction accuracy of the temperature, salinity and sound speed for our

TABLE I: Prediction Accuracy Results

Depth	Shallow	Deep	All Depth
Temperature MAE (°C)	1.1555	0.1112	0.1866
Temperature Accuracy	94.28 %	99.26 %	98.9 %
Salinity MAE (psu)	0.181	0.0161	0.028
Salinity Accuracy	99.53 %	99.96 %	99.93 %
Speed MAE (m/s)	3.0569	0.3612	0.5556
Speed Accuracy	99.8 %	99.98 %	99.96 %

separate Random Forest models for shallow ($< 30 m$) and deep ($\geq 30 m$) water.

Results in Figure 4a present the boxplots of the prediction error along the water column, clearly showing how a very small error can be achieved with a depth of more than 50 m, while closer to the surface the prediction error increases. This happens because the dynamics of sound speed at the surface is quite different, presenting higher fluctuations than in deep water (see Figure 1). Given these differences, we tried to use two different predictors for deep water and shallow water, i.e., by using two different random forests, one for predicting the sound speed when the depth is more than 30 meters, and one when the depth is less than 30 meters. Results shown in Figure 4b give a performance improvement of 20% in shallow water with respect to using one single random forest trained with all data, still maintaining the same accuracy for deep water.

In order to prove the effectiveness of our model, in Figure 5 we show the sound speed prediction error if we use the sample mean of the sound speed computed for each depthgroup on different time intervals, namely:

- the last year until one month before the prediction, named from here onwards AVG;
- the month before the prediction, named from here onwards LM;
- the same month but the year before the prediction, named from here onwards YB.

While AVG clearly provides a wrong prediction of the

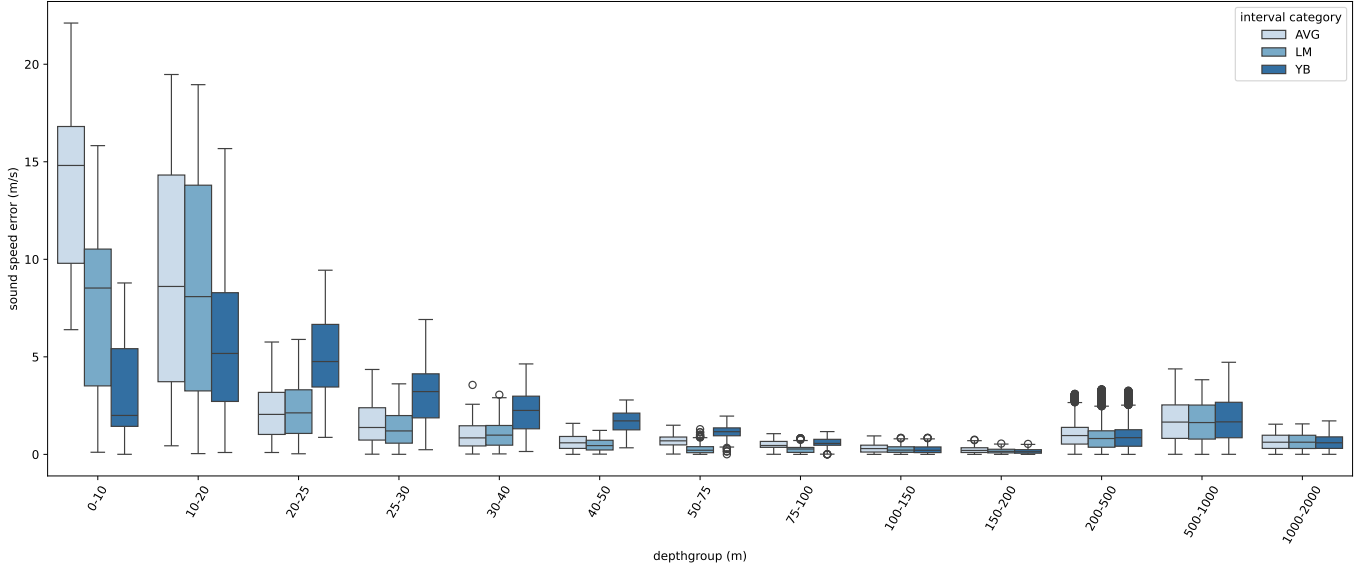


Fig. 5: Boxplots grouped by depth showing the error of the benchmark models.

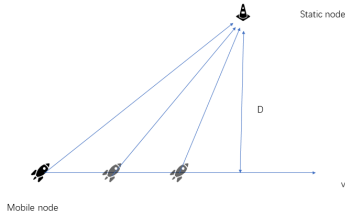


Fig. 6: Uplink Ranging.

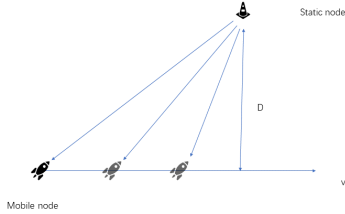


Fig. 7: Downlink Ranging.

sound speed, better results can be obtained with LM and, specially, with YB. Still, even using YB the prediction error is significantly higher than with random forest, especially in shallow water and for a water depth higher than 200 m.

III. ONE-WAY RANGING PROTOCOL

In mobile underwater acoustic communications, the propagation speed of signal is 5 orders of magnitude lower than the speed of EM wave or Optics, and the motion of mobile node can not be ignored. In applications related to ranging, it

is necessary to compensate for the offset of the mobile node during the acoustic signal propagation.

We provide two scenarios of ranging service shown in Figure 6 and Figure 7. In the first scenario, the mobile nodes proactively send packets to static nodes to provide updates about their mobility and position information. In the other one, the mobile nodes passively receive packets from static nodes to estimate their own mobility and position information. In both scenarios we use our precise estimation of sound speed c mentioned above. Table II describes the parameters of the ranging protocol.

TABLE II: Parameters Description

Name	Description
v	velocity of the mobile node
D	distance between the static node and the trajectory of the mobile node
c	speed of sound underwater
t_0	timestamp for the first packet transmission
t_{slot}	slot duration from the sender
t_1	time of arrival for the first packet
t_2	time of arrival for the second packet
t_3	time of arrival for the third packet

We assume that one of the ranging parties is a static node and the other is a mobile node. If there are two moving nodes, we use one of them as a static reference to estimate the relative motion. Our current algorithm takes the motion during the ranging process as moving along a straight line with a constant velocity v . The distance between the static node and the trajectory of the mobile node is D . In uplink ranging, the mobile node sends two packets of the same duration t_{pkt} . In downlink ranging, the static node sends two packets of the same duration t_{pkt} . We utilize this transmission of two packets as multiple measurements. With these ranging data

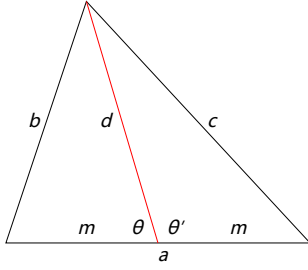


Fig. 8: Apollonius Theorem.

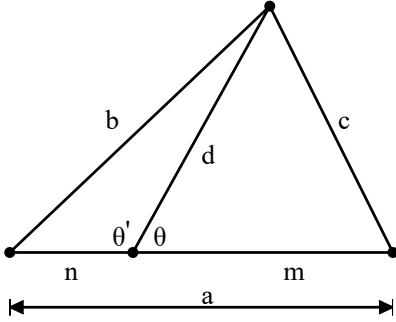


Fig. 9: Stewarts Theorem.

we can derive the relative velocity of the mobile node and the distance between the static node and the trajectory.

The idea is to construct the structure of the center line of the triangle. The mobile node moves in a fixed direction and sends three data packets or pulse signals towards the static node. Such a geometric relationship forms the structure of Stewart's theorem [15]. If the mobile node moves the same distance during the transmission interval, it forms the structure of Apollonius' theorem, which makes the calculation simpler.

In Figure 8, let a , b , c be the lengths of the sides of a triangle. Let d be the length of a cevian to the side of length a . If the cevian divides the side of length a into two segments of lengths m and n , with m adjacent to c and n adjacent to b , then Stewart's theorem states that

$$b^2m + c^2n = a(d^2 + mn). \quad (2)$$

In Figure 9, let the triangle have sides a , b , c with a median d drawn to side a . Let m be the length of the segments of a formed by the median, so m is half of a , then Apollonius's theorem states that

$$b^2 + c^2 = 2(d^2 + m^2). \quad (3)$$

In the uplink ranging process, the mobile node transmits three packets or three pulse signals to the static node to allow the static node to calculate the speed of the mobile node and the distance between the two nodes. The three packets are transmitted one by one and equally spaced. We consider the mobile node to be moving at a constant speed during the

ranging process. The mobile node as the sender travels the same distance between two transmissions. With timestamp of transmissions and arrival times, the travel time of each packet can be calculated on the static node's side. p_1 , p_2 and p_3 are the distances along the propagation path of the three packets:

$$p_1 = (t_1 - t_0) c \quad (4)$$

$$p_2 = (t_2 - t_0 - t_{slot}) c \quad (5)$$

$$p_3 = (t_3 - t_0 - 2t_{slot}) c. \quad (6)$$

According to Apollonius's Theorem,

$$2p_2^2 + 2v^2t_{slot}^2 = p_1^2 + p_3^2 \quad (7)$$

We can solve for the speed of the mobile node:

$$v = \frac{1}{t_{slot}} \sqrt{\frac{1}{2}p_1^2 + \frac{1}{2}p_3^2 - p_2^2}. \quad (8)$$

At a certain time t after the third arrival, before the speed of the mobile node changes, we can solve the ranging r at time t with Stewart's Theorem:

$$p_2^2 (t - t_0 - 2t_{slot}) v + r^2 t_{slot} v = (t - t_0 - t_{slot}) v (p_3^2 + t_{slot} v^2 (t - t_0 - 2t_{slot})). \quad (9)$$

$$r^2 = \frac{(t - t_0 - t_{slot}) (p_3^2 + t_{slot} v^2 (t - t_0 - 2t_{slot}))}{t_{slot} \frac{p_2^2 (t - t_0 - 2t_{slot})}{t_{slot}}} \quad (10)$$

In the downlink ranging process, the static node transmits three packets or three pulse signals to the mobile node to allow the mobile node to calculate its own speed and the distance between the two nodes. The three packets are transmitted one by one within the same interval. Due to mobility, the intervals of the arrivals of the three packets are not the same but with timestamp of transmissions and arrival times, the travel time of each packet can be calculated on the mobile node's side:

$$p_1 = (t_1 - t_0) c \quad (11)$$

$$p_2 = (t_2 - t_0 - t_{slot}) c \quad (12)$$

$$p_3 = (t_3 - t_0 - 2t_{slot}) c. \quad (13)$$

We can apply Stewart's Theorem to solve for the speed of the mobile node:

$$p_1^2 (t_3 - t_2) v + p_3^2 (t_2 - t_1) v = (p_2^2 + v^2 (t_3 - t_2) (t_2 - t_1)) (t_3 - t_1) v \quad (14)$$

$$v^2 = \frac{p_1^2}{(t_3 - t_1) (t_2 - t_1)} + \frac{p_3^2}{(t_3 - t_1) (t_3 - t_2)} - \frac{p_2^2}{(t_3 - t_2) (t_2 - t_1)}. \quad (15)$$

At a certain time t after the third arrival, before the speed of the mobile node changes, we can solve for the ranging r at time t with Stewart’s Theorem:

$$r^2 (t_3 - t_2) v + p_2^2 (t - t_3) v = (p_3^2 + v^2 (t_3 - t_2) (t - t_3)) (t - t_2) v \quad (16)$$

$$r^2 = \frac{(t - t_2) p_3^2}{t_3 - t_2} - \frac{(t - t_3) p_2^2}{t_3 - t_2} + (t - t_2) (t - t_3) v^2 \quad (17)$$

TABLE III: Simulation settings

Parameter	Value
Number of nodes (N)	2
Node speed	2 m/s
TDMA Slot time	0.2 s
Source level	200 dB re 1 μ Pa 1 m
Water depth	21 m / 355 m
Central frequency	65 kHz
Bandwidth	30 kHz
Bitrate	1000 bps
Packet size	8 bytes
Modulation	BPSK
Wind speed	1 m/s
Shipping level	1
Practical spreading	1.5
Interference model	DESERT “meanpower” model, considered at SINR

IV. SIMULATION RESULTS

In this section we describe the simulation setup (Section IV-A) used to evaluate the ranging algorithm, and the simulation results (Section IV-B) that show the effectiveness of the proposed solution and how important it is to have a good estimate of the sound speed when ranging and localization tasks are performed.

A. Simulation Scenario and Settings

Our simulation was performed within the DESERT Underwater framework [9]. The setup includes simulation depths of 21 and 355 meters to show the performance of the benchmarks and our solution at different depths. We simulate one static node and one mobile node. The mobile node starts from 750 m away from the static node and moves on a straight line at a constant speed of 2 m/s. The distance D between the trajectory and the static node is 500 m and the maximum ranging distance is 2500 m. We set up two scenarios for the simulation. One is uplink, where the mobile node sends packets to the static node and the static node performs computation of the ranging and speed of the mobile node. The other is downlink, where the static node sends packets to the mobile node and the mobile node performs the calculation. The packet transmission follows a slotted schedule. The slot duration is 0.2 s. From each beginning of the first three slots, we transmit one packet of 8 Bytes. We set the sound speed in the simulation as the

measured value on July 17, 2023 and August 17, 2023. We feed the ranging algorithm with our sound speed predictions of the days for each depth and compare the results with the benchmarks.

B. Results

We pick two dates and two depths in the test dataset of sound speed. Compared with the actual distances, we show in Figure 10 that the ranging errors with our predicted sound speeds are significantly smaller than the benchmarks. With just one run of our algorithm at a cost of one propagation delay plus twice a variable slot duration according to the minimum packet size, we are able to maintain an efficient ranging service for both uplink and downlink.

In Figure 10a and Figure 10b, the errors in all categories are larger than those in Figure 10c and Figure 10d, because both spatial and temporal variations of sound speed in shallow water are more severe. With our solution, we managed to control the error in ranging for 2500 m within 2 m.

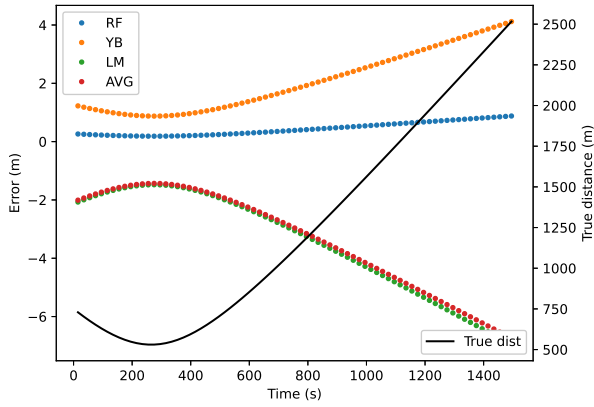
V. CONCLUSION AND FUTURE WORK

This paper presents a one-way travel time ranging protocol for low-cost underwater acoustic network where nodes, instead of using CTD or velocity meter sensors to directly measure the sound speed, are equipped with a machine learning algorithm trained with environmental data usually used for meteorology and retrieved close to the deployment area. Results show how precise prediction of sound speed affects the accuracy of a ranging protocol. Our solution achieves good accuracy as a joint ranging and node speed estimation with minimum channel resource occupation.

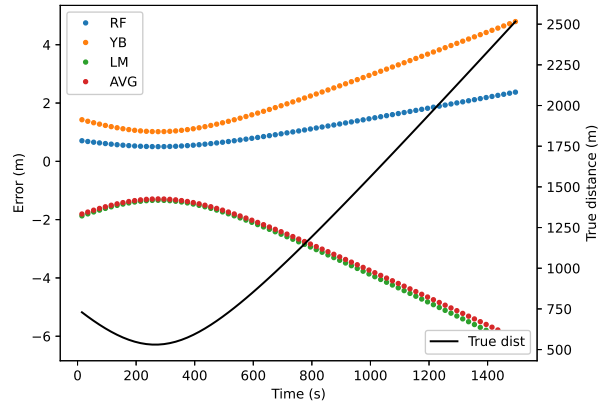
Future work will focus on real field tests proving whether this solution can be applied to a real system.

REFERENCES

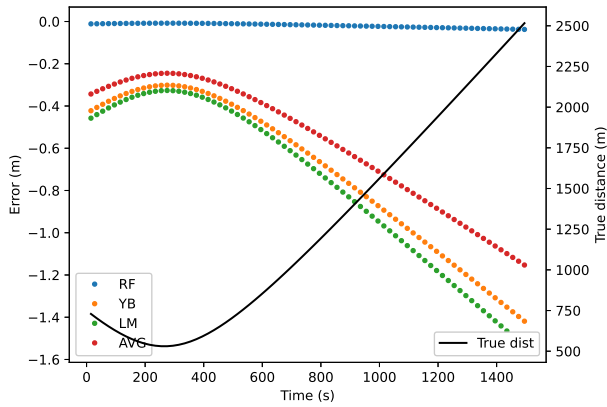
- [1] B. T. Champion and M. A. Joordens, “Underwater swarm robotics review,” in *10th System of Systems Engineering Conference (SoSE)*, 2015, pp. 111–116.
- [2] G. Han, J. Jiang, L. Shu, Y. Xu, and F. Wang, “Localization algorithms of underwater wireless sensor networks: A survey,” *Sensors*, vol. 12, no. 2, pp. 2026–2061, 2012. [Online]. Available: <https://www.mdpi.com/1424-8220/12/2/2026>
- [3] J. Liu, Z. Wang, M. Zuba, Z. Peng, J.-H. Cui, and S. Zhou, “DA-Sync: A Doppler-Assisted Time-Synchronization Scheme for Mobile Underwater Sensor Networks,” *IEEE Transactions on Mobile Computing*, vol. 13, no. 3, pp. 582–595, March 2014.
- [4] T. Stojimirovic and B.-C. Renner, “Accuracy of TWR-Based Ranging and Localization in Mobile Acoustic Underwater Networks,” in *Fifth Underwater Communications and Networking Conference (UComms)*, 2021, pp. 1–5.
- [5] M. Stojanovic and J. Preisig, “Underwater acoustic communication channels: Propagation models and statistical characterization,” *IEEE Communications Magazine*, vol. 47, no. 1, pp. 84–89, January 2009.
- [6] “CTD Instruments & Environmental Sensors,” Last time accessed: Jan. 2024. [Online]. Available: <https://www.valeport.co.uk/product-types/ctd-environmental/>
- [7] “miniSVS Sound Velocity Sensor,” Last time accessed: Jan. 2024. [Online]. Available: <https://www.valeport.co.uk/products/minisvs-sound-velocity-sensor/>
- [8] E. Coccolo, F. Campagnaro, D. Tronchin, A. Montanari, R. Francescon, L. Vangelista, and M. Zorzi, “Underwater Acoustic Modem for a MORphing Distributed Autonomous Underwater Vehicle (MODA),” in *IEEE/MTS OCEANS - Chennai, 2022*, pp. 1–8.



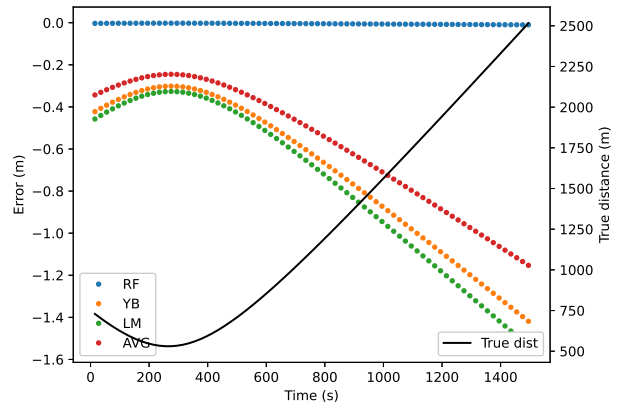
(a) Depth 21 m, July 17.



(b) Depth 21 m, August 17.



(c) Depth 355 m, July 17.



(d) Depth 355 m, August 17.

Fig. 10: Performance of the ranging with different estimates of the sound speed for different depths and dates.

- [9] F. Campagnaro *et al.*, “The DESERT underwater framework v2: Improved capabilities and extension tools,” in *Proc. Ucomms*, Lerici, Italy, Sep. 2016.
- [10] “What is argo?” <https://argo.ucsd.edu>, Last time accessed: Jan. 2024.
- [11] “Oceanops,” <https://www.ocean-ops.org>, Last time accessed: Oct. 2023.
- [12] “Argo-italy,” <https://argo.ogs.it>, Last time accessed: Jan. 2024.
- [13] A. B. Riaz Ahmed, M. Younis, M. H. De Leon, “Machine Learning Based Sound Speed Prediction for Underwater Networking Applications,” in *IEEE International Conference on Distributed Computing in Sensor Systems (DCOSS)*, Pafos, Cyprus, July 2021.
- [14] W. D. Wilson, “Nine-term equation for sound speed in the oceans,” *Acoustic Society of America*, vol. 32, no. 6, p. 641–644, 1960.
- [15] L. Bulwahn, “Stewart’s Theorem and Apollonius’ Theorem,” *Archive of Formal Proofs*, July 2017, https://isa-afp.org/entries/Stewart_Apollonius.html, Formal proof development.